



TITLE:

Data in support of crystal structures of highly-ordered long-period stacking-ordered phases with 18R, 14H and 10H-type stacking sequences in the Mg-Zn-Y system

AUTHOR(S):

Kishida, Kyosuke; Nagai, Kaito; Matsumoto, Akihide; Inui, Haruyuki

CITATION:

Kishida, Kyosuke ...[et al]. Data in support of crystal structures of highly-ordered long-period stacking-ordered phases with 18R, 14H and 10H-type stacking sequences in the Mg-Zn-Y system. Data in Brief 2015, 5: 314-320

ISSUE DATE:

2015-12

URL:

<http://hdl.handle.net/2433/217461>

RIGHT:

© 2015 The Authors. Published by Elsevier Inc. This is an open access article under the CC BY license (<http://creativecommons.org/licenses/by/4.0/>).



ELSEVIER

Contents lists available at ScienceDirect

Data in Brief

journal homepage: www.elsevier.com/locate/dib

CrossMark

Data Article

Data in support of crystal structures of highly-ordered long-period stacking-ordered phases with 18R, 14H and 10H-type stacking sequences in the Mg–Zn–Y system

Kiyosuke Kishida^{a,b,*}, Kaito Nagai^a, Akihide Matsumoto^a, Haruyuki Inui^{a,b}^a Department of Materials Science and Engineering, Kyoto University, Sakyo-ku, Kyoto 606-8501, Japan^b Center for Elements Strategy Initiative for Structural Materials (ESISM), Kyoto University, Sakyo-ku, Kyoto 606-8501, Japan

ARTICLE INFO

Article history:

Received 10 August 2015

Received in revised form

3 September 2015

Accepted 7 September 2015

Available online 25 September 2015

ABSTRACT

The crystal structures of highly-ordered Mg–Zn–Y long-period stacking-ordered (LPSO) phases with the 18R, 14H and 10H-type stacking sequences have been investigated by atomic-resolution scanning transmission electron microscopy (STEM) and transmission electron microscopy (Kishida et al., 2015) [1]. This data article provides supporting materials for the crystal structure analysis based on the crystallographic theory of the order–disorder (OD) structure and the crystallographic information obtained through the structural optimization for various simple polytypes of the highly-ordered Mg–Zn–Y LPSO phases with the 18R, 14H and 10H-type stacking sequences by first-principles density functional theory (DFT) calculations.

© 2015 The Authors. Published by Elsevier Inc. This is an open access article under the CC BY license

(<http://creativecommons.org/licenses/by/4.0/>).

Specifications Table

Subject area	Materials Science
More specific subject area	Magnesium alloys, crystal structure, order–disorder (OD) structure

DOI of original article: <http://dx.doi.org/10.1016/j.actamat.2015.08.004>

* Corresponding author.

E-mail address: kishida.kyosuke.6w@kyoto-u.ac.jp (K. Kishida).<http://dx.doi.org/10.1016/j.dib.2015.09.005>2352-3409/© 2015 The Authors. Published by Elsevier Inc. This is an open access article under the CC BY license (<http://creativecommons.org/licenses/by/4.0/>).

Type of data	Text, Image (scanning electron microscopy (SEM)), transmission electron microscopy (TEM)), Table, Crystallographic information in cif format
How data was acquired	Scanning electron microscope (JEOL JSM-7001FA), Transmission electron microscope (JEOL JEM-2100F), WinHREM software package [3] and the Vienna Ab initio simulation package (VASP) [4–6].
Data format	Raw, Analyzed
Experimental factors	High-frequency induction melting in an argon atmosphere
Experimental features	Heat-treated at 500 °C for 72 and 300 h.
Data source location	Department of Materials Science and Engineering, Kyoto University, Kyoto, Japan
Data accessibility	Data is available with this article.

Value of the data

- The crystallographic data is essential for the investigations of the crystal structures, defect structures and crystallographic orientations of the Mg–Zn–Y LPSO phases by transmission electron microscopy (TEM), scanning transmission electron microscopy (STEM), electron backscatter diffraction (EBSD) in SEM and the other diffraction analysis methods.
- The results of the structural optimization provide useful information for understanding the influences of the stacking relationships between the adjacent structural blocks as well as the additional atoms in Zn_6Y_8 atomic clusters on the formation energies of the Mg–Zn–Y LPSO/OD phases and also the phase relationships in the Mg–Zn–Y ternary system.
- The results of diffraction analysis in TEM provides useful information about how the crystal structure evolution can be detected in selected area electron diffraction (SAED) patterns.

1. SEM observations

Typical SEM back-scattered electron (BSE) images for alloys A (nominal composition: Mg – 8.3 at% Zn – 11.1 at% Y) and B (nominal composition: Mg – 10.0 at% Zn – 13.3 at% Y) after the heat treatment at 500 °C for 72 h are shown in Fig. 1(a) and (b), respectively. Although the nominal compositions were chosen to obtain single-phase ingots of the fully ordered phases with 18R- and 10H-LPSO phases, both ingots contain Zn,Y-rich precipitates, which are imaged as the brightest regions in Fig. 1. EDS analysis in the SEM has indicated that the overall compositions for alloys A and B are deviated slightly to the Mg-poor compositions of Mg – 9.2 ± 0.3 at% Zn – 11.2 ± 0.3 at% Y and Mg – 11.4 ± 0.2 at% Zn – 12.8 ± 0.1 at% Y, respectively. The brightest regions in Fig. 1 possess an approximate chemical compositions of Mg – 47.0 ± 0.6 at% Zn – 26.6 ± 0.2 at% Y, which are inferred to be W phase previously reported [2]. The SEM-BSE images for alloys A and B heat-treated at 500 °C for about 300 h indicate that major regions for both alloys still exhibit compositional heterogeneity, which could not be eliminated even after the prolonged heat treatment at 500 °C (Fig. 1(c) and (d)).

2. Selected area electron diffraction (SAED) patterns of highly-ordered Mg–Zn–Y LPSO/OD phases

The crystal structure transformation from one-dimensionally disordered structure into the MDO_2 polytype (2M_1 , space group: $C2/c$ (15)) belonging to the OD groupoid family of the C_3 -type has been confirmed for the Mg–Zn–Y LPSO/OD phase with the 18R-type stacking sequence through the analysis of the atomic resolution STEM images [1]. Fig. 2 shows the corresponding experimental SAED patterns

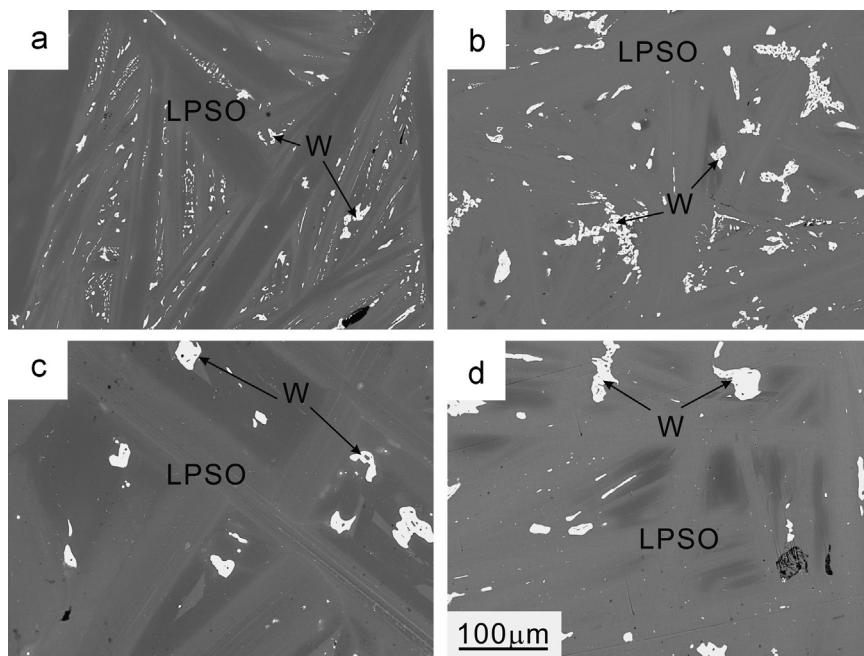


Fig. 1. SEM back-scattered electron (BSE) images of alloys (a, c) A and (b, d) B heat-treated at 500 °C for (a, b) 72 h and (c, d) 300 h.

of the $\langle 1\bar{1}00 \rangle$ and $\langle 2\bar{1}\bar{1}0 \rangle$ incidences taken from the 18R-type Mg–Zn–Y LPSO/OD phase heat-treated at 500 °C for 72 and 300 h. For simplicity, indices to express directions and planes for the LPSO phases are referred to as those of the parental Mg phase with the hcp structure unless otherwise noted. Each of the SAED patterns was obtained from a circular area with an approximately 120 nm in diameter in a grain of 18R-type Mg–Zn–Y LPSO/OD phase. In the SAED pattern taken from the LPSO/OD phase heat-treated at 500 °C for 72 h, the sharp diffraction spots in the reciprocal lattice rows of $n/6 \langle 11\bar{2} \rangle^*$ ($n=0$ and 6) and $n/2 \langle 01\bar{1} \rangle^*$ ($n=\text{even integers}$) and intense streaks in the reciprocal lattice rows of $n/6 \langle 11\bar{2} \rangle^*$ ($n=1, 2, 3, 4$ and 5) and $n/2 \langle 01\bar{1} \rangle^*$ ($n=\text{odd integers}$) are observed to be coexisted, which is one of the characteristics of the OD structure with one dimensional stacking disorder and can be used as a guide for distinguishing the OD structure with the other crystal structure types, i.e., LPSO and fully-ordered structures by the diffraction analysis in TEM [1]. In contrast, only sharp diffraction spots are observed after the heat-treatment at 500 °C for 300 h, reflecting the crystal structure transformation into a fully ordered structure. The SAED patterns taken from the specimens heat-treated for 300 h are compared with those calculated using the crystallographic parameters given in [1, Table 3] (CIF: 18R-stable_C3-2M1.cif in [Supplementary material](#) in this paper) with the WinHREM software package (Fig. 2) [3]. Since the domain structure composed of three differently oriented domains is formed in the 18R-type Mg–Zn–Y LPSO/OD phase [1], the experimental SAED patterns of the $\langle 1\bar{1}00 \rangle$ and $\langle 2\bar{1}\bar{1}0 \rangle$ incidences coincide well with those obtained after superposing the three SAED patterns calculated for the three different incidences, namely those of $[100]_{2M_1} - [\bar{1}10]_{2M_1} - [\bar{1}\bar{1}0]_{2M_1}$ and $[010]_{2M_1} - [310]_{2M_1} - [\bar{3}10]_{2M_1}$, respectively, where the indices with the subscript $2M_1$ are referred to the MDO_2 ($2M_1$) monoclinic cell.

3. First-principles DFT calculations

Structural optimization for various simple polytypes are conducted using the Vienna Ab-initio Simulation Package (VASP) [4]. These simple polytypes are derived based on the crystallographic theory of the order–disorder (OD) structure and are designated as those with the maximum degree of order (MDO polytypes) [1]. The Perdew–Burke–Ernzerhof (PBE) gradient approximation (GGA-PBE) is utilized to treat the exchange–correlation functional [5]. An energy cutoff is set to be 400 eV and Monkhorst-Pack k-point meshes of $6 \times 4 \times 4$ (for 1M cells), $6 \times 4 \times 2$ (for 2M, 2O and 1A calculated with double-sized C-centered cells) and a gamma-centered k-point mesh of $6 \times 6 \times 2$ (for 2H-type hexagonal cells) are used throughout the calculations [6]. The geometric optimization is terminated when the residual forces become less than 0.01 eV/Å.

Table 1 summarizes the formation energy ΔE_{form} and stability factor ΔE_{stab} defined by Saal and Wolverton [7] as well as lattice constants obtained by the first-principle calculations. The ΔE_{form} and ΔE_{stab} values are evaluated according to the following equations:

$$\Delta E_{\text{form}} = E_{\text{tot}}(\text{Mg}_l\text{Zn}_m\text{Y}_n) - \frac{lE_{\text{tot}}(\text{Mg}) + mE_{\text{tot}}(\text{Zn}) + nE_{\text{tot}}(\text{Y})}{l + m + n}, \quad (1)$$

$$\Delta E_{\text{stab}}(\text{Mg}_l\text{Zn}_m\text{Y}_n) = E_{\text{tot}}(\text{Mg}_l\text{Zn}_m\text{Y}_n) - E_{\text{CH}}(\text{Mg}_l\text{Zn}_m\text{Y}_n), \quad (2)$$

where $E_{\text{tot}}(i)$ is the total energy per atom of the structure (i) and $E_{\text{CH}}(\text{Mg}_l\text{Zn}_m\text{Y}_n)$ is the energy of the convex hull at the composition of the LPSO phase. We assume that the convex hull is composed of Mg, MgZnY and Mg_3Y as proposed by Saal and Wolverton [7].

The crystallographic information files (CIF) for the optimized MDO polytypes of the 18R-, 14H- and 10H-type Mg–Zn–Y LPSO/OD phases with or without an additional atoms at the central site of each Zn_6Y_8 atomic cluster are provided as the [supplementary materials](#).

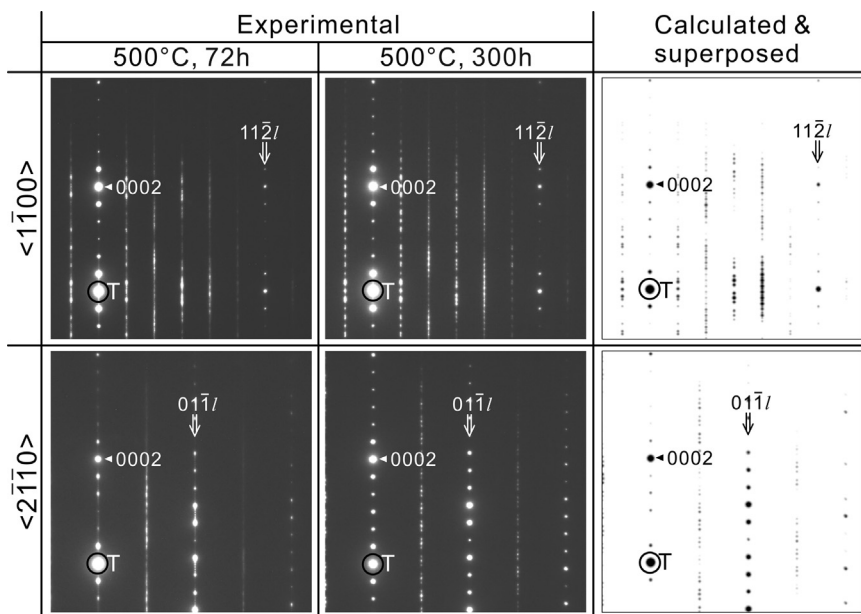


Fig. 2. Experimental and calculated SAED patterns for the C_3 -MDO₂ polytype of the 18 R-type Mg–Zn–Y LPSO/OD phase in alloy B heat-treated at 500 °C for 72 and 300 h.

Table 1Formation energy ΔE_{form} , stability factor ΔE_{stab} and lattice parameters for some MDO polytypes of Mg–Zn–Y LPSO/OD phases. c_{SB} correspond to the height of the structural block.

Stacking sequence type	Stacking relation	MDO polytypes	Space group	Additional atom	Formation energy, ΔE_{form} (meV/atom)	Stability factor, ΔE_{stab} (meV/atom)	Nearest out-of-plane inter-cluster distance (Å)	Lattice parameters						c_{SB} (Å)
								a (Å)	b (Å)	c (Å)	α (°)	β (°)	γ (°)	
10 <i>H</i>	A_1	$2H$	$P6_3/mcm$	–	–81.9	18.7	13.04	11.21	–	26.08	90	90	120	13.04
				Mg	–110.9	–12.0	13.07	11.20	–	26.13	90	90	120	13.07
				Zn	–105.8	1.7	13.05	11.18	–	26.10	90	90	120	13.05
				Y	–111.0	–6.1	13.07	11.23	–	26.14	90	90	120	13.07
	A_2	$2H$	$P6_322$	–	–82.7	17.9	14.56	11.20	–	26.10	90	90	120	13.05
				Mg	–111.9	–13.0	14.58	11.20	–	26.13	90	90	120	13.07
				Zn	–107.0	0.5	14.55	11.18	–	26.08	90	90	120	13.04
				Y	–111.2	–6.1	14.61	11.23	–	26.17	90	90	120	13.09
	A_3	$2O$	$Cmce$	–	–83.2	17.4	14.23	19.40	11.18	26.16	90	90	90	13.08
				Mg	–112.3	–13.3	14.22	19.38	11.20	26.14	90	90	90	13.07
				Zn	–107.3	0.1	14.20	19.35	11.18	26.11	90	90	90	13.05
				Y	–111.1	–6.2	14.25	19.43	11.23	26.19	90	90	90	13.10
	A_4	$2O$	$C222_1$	–	–82.7	17.9	13.48	11.18	19.37	26.18	90	90	90	13.09
				Mg	–111.7	–12.8	13.47	11.19	19.38	26.16	90	90	90	13.08
				Zn	–106.8	0.6	13.46	11.17	19.35	26.13	90	90	90	13.07
				Y	–111.0	–6.1	13.49	11.22	19.44	26.19	90	90	90	13.10
18 <i>R</i>	C_1	$1M$	$C2/m$	–	–99.8	–16.0	16.09	11.16	19.36	16.09	90	103.54	90	15.65
				Mg	–124.7	–42.1	16.08	11.16	19.37	16.08	90	103.59	90	15.63
				Zn	–120.1	–30.3	16.07	11.15	19.34	16.07	90	103.53	90	15.62
				Y	–123.5	–35.8	16.12	11.19	19.40	16.12	90	103.59	90	15.67
		$2M$	$C2/c$	–	–99.9	–16.0	16.08	11.17	19.34	31.52	90	96.87	90	15.65
				Mg	–124.8	–42.1	16.07	11.17	19.36	31.50	90	96.87	90	15.64
				Zn	–120.1	–30.3	16.06	11.15	19.33	31.48	90	96.85	90	15.63
				Y	–123.4	–35.8	16.11	11.19	19.39	31.56	90	96.87	90	15.67
	C_2	$1M$	$C2/m$	–	–99.7	–15.9	15.74	11.17	19.36	15.74	90	96.87	90	15.62
				Mg	–124.2	–41.5	15.74	11.17	19.38	15.74	90	96.91	90	15.62
				Zn	–119.5	–29.7	15.73	11.16	19.35	15.73	90	96.88	90	15.61
				Y	–123.6	–36.0	15.76	11.20	19.42	15.76	90	96.92	90	15.64
		$2M$	$C2/c$	–	–99.9	–16.1	15.73	11.17	19.37	31.31	90	93.48	90	15.62
				Mg	–124.2	–41.6	15.74	11.17	19.36	31.32	90	93.45	90	15.63
				Zn	–119.5	–29.7	15.73	11.16	19.33	31.29	90	93.44	90	15.62
				Y	–123.6	–36.0	15.76	11.20	19.41	31.36	90	93.49	90	15.65
	C_3	$1A$	$P\bar{1}$	–	–100.0	–16.2	16.40	11.18	11.16	16.40	93.27	103.2	120.0	15.64
				Mg	–124.6	–42.0	16.40	11.18	11.16	16.40	93.32	103.2	120.0	15.64
				Zn	–119.9	–30.1	16.41	11.16	11.15	16.41	93.33	103.2	120.0	15.64
				Y	–123.6	–35.9	16.42	11.22	11.19	16.42	93.22	103.3	120.0	15.65

14 H	A ₁	2M ₁	C2/c	–	–100.0	–16.2	16.39	11.17	19.37	31.32	90	93.53	90	15.63
				Mg	–124.7	–42.0	16.38	11.18	19.37	31.31	90	93.41	90	15.62
				Zn	–119.9	–30.1	16.37	11.16	19.34	31.29	90	93.43	90	15.61
				Y	–123.5	–35.9	16.41	11.20	19.42	31.36	90	93.45	90	15.65
		2M ₂	C2/c	–	–100.0	–16.2	16.39	11.17	19.36	31.48	90	96.84	90	15.63
				Mg	–124.6	–41.9	16.38	11.18	19.36	31.46	90	96.81	90	15.62
				Zn	–119.9	–30.1	16.37	11.16	19.33	31.45	90	96.83	90	15.61
				Y	–123.5	–35.9	16.41	11.21	19.41	31.52	90	96.83	90	15.65
		2M ₃	C2/c	–	–100.1	–16.3	16.39	11.17	19.36	31.32	90	93.40	90	15.63
				Mg	–124.6	–41.9	16.38	11.17	16.37	31.31	90	93.42	90	15.63
				Zn	–119.9	–30.1	16.37	11.16	16.34	31.29	90	93.41	90	15.62
				Y	–123.5	–35.9	16.41	11.19	16.42	31.36	90	93.44	90	15.65
	A ₂	2H	P6 ₃ /mcm	–	–61.4	10.4	18.18	11.17	–	36.36	90	90	120	18.18
				Mg	–82.5	–11.5	18.20	11.17	–	36.40	90	90	120	18.20
				Zn	–78.7	–1.6	18.19	11.15	–	36.38	90	90	120	18.19
				Y	–82.3	–7.0	18.22	11.19	–	36.43	90	90	120	18.22
		2H	P6 ₃ 22	–	–61.3	10.5	19.29	11.17	–	36.37	90	90	120	18.18
				Mg	–82.6	–11.6	19.29	11.17	–	36.36	90	90	120	18.18
				Zn	–78.8	–1.7	19.27	11.16	–	36.33	90	90	120	18.17
				Y	–81.8	–6.5	19.31	11.19	–	36.40	90	90	120	18.20
		2O	Cmce	–	–61.2	10.7	19.03	19.37	11.15	36.40	90	90	90	18.20
				Mg	–82.4	–11.4	19.03	19.38	11.15	36.39	90	90	90	18.20
				Zn	–78.7	–1.6	19.02	19.35	11.13	36.38	90	90	90	18.19
				Y	–81.6	–6.3	19.06	19.40	11.18	36.45	90	90	90	18.23
	A ₄	2O	C222 ₁	–	–61.3	10.6	18.48	11.15	19.37	36.40	90	90	90	18.20
				Mg	–82.3	–11.3	18.48	11.16	19.36	36.39	90	90	90	18.20
				Zn	–78.5	–1.4	18.47	11.15	19.33	36.37	90	90	90	18.19
				Y	–81.8	–6.5	18.51	11.18	19.40	36.45	90	90	90	18.23

Acknowledgments

This work was supported by Grants-in-Aid for Scientific Research from the Ministry of Education, Culture, Sports, Science and Technology (MEXT), Japan (Nos. 23360306, 23109002, 26109712 and 26289258) and in part by the Elements Strategy Initiative for Structural Materials (ESISM) from MEXT, Japan.

Appendix A. Supplementary material

Supplementary data associated with this article can be found in the online version at <http://dx.doi.org/10.1016/j.dib.2015.09.005>.

References

- [1] K. Kishida, K. Nagai, A. Matsumoto, A. Yasuhara, H. Inui, Crystal structures of highly-ordered long-period stacking-ordered phases with 18R, 14H and 10H-type stacking sequences in the Mg–Zn–Y system, *Acta Mater.* 99 (2015) 228–239.
- [2] A. Hamaya, T. Horiuchi, Y. Oohira, S. Minamoto, S. Miura, N. Sakaguchi, Experimental study on phase equilibria in the vicinity of X, W and H phases in the Mg–Zn–Y ternary system, *Mater. Trans.* 54 (2013) 641–646.
- [3] K. Ishizuka, A practical approach for STEM image simulation based on the FFT multislice method, *Ultramicroscopy* 90 (2002) 71–83.
- [4] G. Kresse, J. Furthmüller, Efficient iterative schemes for ab initio total-energy calculations using a plane-wave basis set, *Phys. Rev. B* 54 (1996) 11169–11186.
- [5] J.P. Perdew, K. Burke, M. Ernzerhof, Generalized gradient approximation made simple, *Phys. Rev. Lett.* 77 (1996) 3865–3868.
- [6] H.J. Monkhorst, J.D. Pack, Special points for Brillouin-zone integration, *Phys. Rev. B* 13 (1976) 5188–5192.
- [7] J.E. Saal, C. Wolverton, Thermodynamic stability of Mg-based ternary long-period stacking ordered structures, *Acta Mater.* 68 (2014) 325–338.